A Low-cost Passive Visible Light Communication System

Qing Wang
IMDEA Networks Institute
qing.wang@imdea.org

Marco Zuniga
Delft University of Technology
m.a.zunigazamalloa@tudelft.nl

Domenico Giustiniano
IMDEA Networks Institute
domenico.giustiniano@imdea.org

arXiv:1512.04362v2 [cs.NI] 26 Jan 2016

Abstract

In this work, we propose a new communication system for illuminated areas, indoors and outdoors. Light sources in our environments – such as light bulbs or even the sun – are our signal emitters, but we do not modulate data using the light source. We instead propose that the environment itself modulates the light signals: if any mobile element 'wears' a pattern consisting of distinctive reflecting surfaces, a receiver could decode the disturbed light signals to read *passive* information. Mobility here is key to transfer the information to the destination, since objects or people passing by will disturb the surrounding light signals. Like barcode readers in our stores, light sources in our environments could be leveraged to monitor logistics and activities in cities and buildings. Achieving this vision requires a deep understanding of a new type of communication channel. Many parameters can affect the performance of passive communication signals based on visible light: the specific patterns of the reflective surfaces, the surrounding light intensity and the speed of the mobile objects, to name a few. In this position paper, we present an initial experimental and analytical approach to tackle some of the main challenges associated with realizing a passive communication channel with visible light.

1. INTRODUCTION

The basic functional blocks of a digital communication system –the information source, the transmitter, the channel and the receiver– are the foundation of today's wireless communication [12]. The idea behind this well-established concept is that information sources should use the transmitter to modulate data, so it can travel through the channel and be decoded by the intended receiver. This type of communication is a modern concept. In the past, when no advanced transmitters were available, people used the environment as both the channel and the information source. In the early 1900's heliographs (mirrors) were a widely popular tool used by many armies for long distance wireless communication.

Inspired by this old communication concept, and motivated by the fundamental principles of two emerging areas, visible light communication and backscatter communication, we propose a new flowchart for a *passive* communication system based on visible light, as illustrated in Fig. 1. Our communication system is composed of three basic elements. First, transmitters, which could be any *simple unmodulated* light source such as LED bulbs, incandescent bulbs or the sun. Second, receivers, which are small boxes containing at least one photosensor to measure the impinging light intensity. Third, 'packets', which are surfaces containing different

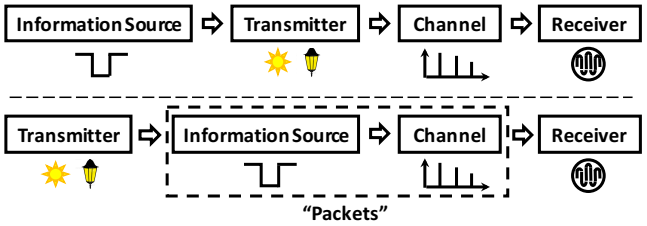

Figure 1: Flowchart of classic communication (top) and our proposal (bottom).

reflective materials, as described later. This simple system would enable us to decode information in a passive manner from surrounding physical objects, *leading in effect to a sort of city-wide or building-wide barcode reader system to monitor internal events.* To realize this vision however, we need to understand the principles of this new type of communication channel. In this paper we formulate the basic key challenges and preliminary solutions associated with this goal.

2. CHALLENGES

We depict the principles of our communication system in Fig. 2. Mobile objects have embedded messages on their surface in the form of variable reflection patterns, similar to barcodes. The reflective materials could be anything, from a pure mirror (strong reflection perpendicular to the incident light, as in classical heliographs) to a dark and rugged cloth (minimal reflection scattered in all directions). As the object moves, the reflected light beams vary with the reflection rate, thus altering the amount of light impinging towards a particular receiver. The receiver can then decode the incoming signal to obtain information about the object(s) under its field of view. While this idea is simple, putting it in practice requires investigating some fundamental challenges.

Challenge 1: Channel capacity. Any communication system needs to quantify the maximum data rate of its channels. For us, this means understanding how different parameters – such as the width of reflective surfaces and the speed of mobile element– affect the capacity of the passive channel (maximum number of symbols per second at the receiver).

Challenge 2: Channel distortions. Similar to traditional radio systems, our channel will be exposed to significant distortions. For example: fog, humidity, dirt on top of the reflective surfaces and variable speeds of the mobile object will be commonplace phenomena distorting the incoming signal and making it harder to decode.

Challenge 3: 'Packet' collisions. The previous two challenges assume that a single object moves under the field

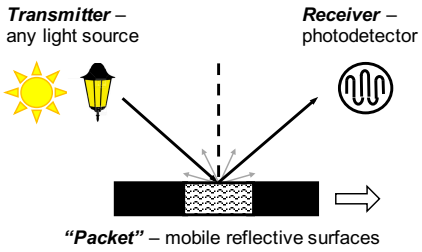

Figure 2: Illustration of the principle of our communication channel.

of view of a receiver. In many applications this assumption will not hold. If several objects move under the field of view, the incoming signal will be the sum of multiple 'out-of-synch' reflections. Leading in fact to the equivalent of packet collisions in radio frequency systems.

Challenge 4: Noise floor. Communication systems based on visible light need to cope with the fact that the surrounding light intensity can change significantly. These changes can modify the 'noise floor' of the channel in a manner that can easily saturate photosensors. Saturating the receiver would make links disappear abruptly.

In Section 3, we look at each one of these challenges from an empirical viewpoint. We showcase the problem at hand and present preliminary solutions for them. In Section 4, we take an analytical viewpoint. We propose a model to derive a theoretical framework for our channel.

3. DECODING INFORMATION: AN EMPIRICAL APPROACH

To investigate the above described challenges empirically, we use three different types of light sources: an LED lamp, standard fluorescent lights in the ceiling of our building, and the sun. Most of our results are based on the LED lamp because it allows us to have controlled and repeatable scenarios. For the receiver, we use the OpenVLC platform, which provides hardware and software solutions for visible light transmission and reception [17]. Given that our channel relies on passive sources, we only use the OpenVLC interfaces related to reception. Before proceeding with our insights, we first introduce some basic information of our system: the coding and decoding of data, and the packet format.

Coding. Our encoding process is passive and can be performed independently by each moving objects. We use two different reflective materials to encode information: aluminum tape, which has a relatively high reflection coefficient and low dispersion (representing the symbol `HIGH`) and black paper napkins, which have a lower reflection coefficient and higher dispersion (representing the symbol `LOW`). The *symbol width*, defined as the width of the material representing that symbol, remains constant within a packet, but different packets can have different symbol widths. To enable an easy and stable decoding at the receivers, we use Manchester encoding to design our codes: a '0'-bit is mapped to symbol sequence `HIGH-LOW`, and a '1'-bit is mapped to `LOW-HIGH`, as shown in the right part of Fig. 3 (Data field).

Packet format. Each moving packet has two fields: preamble and data, as shown in Fig. 3. The preamble is fixed and consists of four symbols `HIGH-LOW-HIGH-LOW`. The Data field comes after the preamble and includes $2N$ symbols (N is a positive integer), representing the modulated

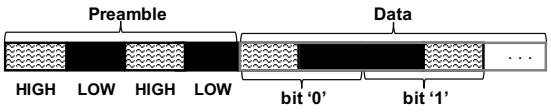

Figure 3: Packet format: Preamble + Data.

N-bit binary data.

Decoding. The receiver decodes information based on Received Signal Strength (RSS). The RSS is perceived as a sequence of `HIGH` and `LOW` symbols, but these symbols can be highly distorted. In the next subsections we propose different mechanisms to process the RSS depending on the level of distortion and interference present in the signal.

3.1 Channel Capacity: The Ideal Scenario

We present some initial experiments aimed at quantifying the channel's capacity. First we describe our decoding method. Then, we assess the impact that the symbol width and the receiver's height have on the channel's throughput.

Decoding. In this subsection we assume that no distortions are present (no dirt or fog) and that packets move at constant speed while passing under the filed of view of the receiver. The speed selected by each packet can be different, but is assumed constant. Unless stated otherwise we use the LED lamp as light source and the experiments are carried in an office where no other sources of light are present: the blinds are closed and light bulbs are turned off. The ground plane where packets move is covered with black papers, to resemble tarmac. To obtain binary data out of the RSS signal, we use two thresholds: one for the magnitude of the RSS signal τ_r (to distinguish whether a symbol is `HIGH` or `LOW`) and one for the time length τ_t (to estimate the duration of a symbol). The thresholds are obtained on a per-packet basis and need to be *highly adaptive* because we do not modulate information with a common transmitter, but we rather let each packet (symbol width, materials used, speed) determine to a large extent the end result of the modulation process.

Due to page limitations, we describe only the basic idea and do not present implementation details used to make the process robust to noise. We first detect the first two peaks and the first valley present in the preamble, points A, B and C in Fig. 4(a). Denoting the tuple $< r_i, t_i >$ as the RSS value and timestamp for point i, the thresholds for the magnitude and period are defined as

$$\tau_r = \frac{(r_A - r_B) + (r_C - r_B)}{2}$$

$$\tau_t = \frac{(t_B - t_A) + (t_C - t_B)}{2}$$

With these thresholds, subsequent RSS measurements are grouped together in windows of length τ_t. If the maximum value in a window is above τ_r we deem the symbol to be `HIGH`, else we deem it to be `LOW`. Figure 4 depicts the RSS for two packets carrying a two-bit (four-symbol) payload: "00" (left) and "10" (right). Both packets have the same symbol width (3 cm). The transmitter and receiver are at a height of 20 cm from the workplace where packets move, and the distance between the transmitter and receiver is 12 cm. For this scenario, the received signals for both packets are clear. It is therefore easy for our decoding method to get accurate values for the thresholds (based on the preamble), and consequently, to decode the information successfully.

The symbol width and channel capacity. Our decoding method enables us to obtain binary data. But a designer

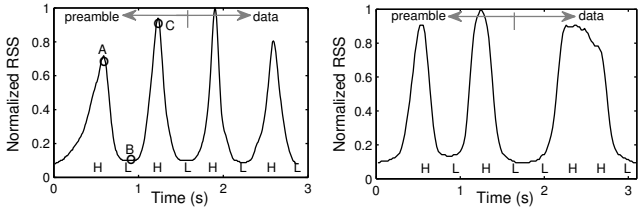

(a) Data='00' ('HLHL') (b) Data='10' ('LHHL')

Figure 4: Signals received at the receiver under ideal scenarios (H represents HIGH; L represents LOW).

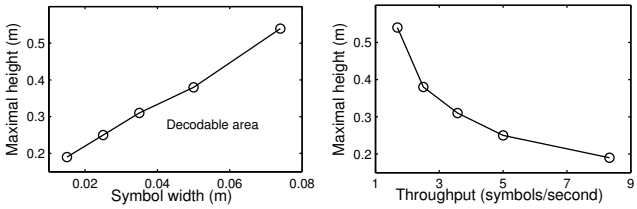

(a) Distance vs. width (b) Distance vs. throughput

Figure 5: Maximal height vs. symbol width and system throughput. Packet's moving speed is 8cm/s.

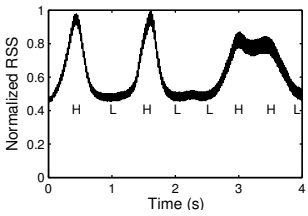

Figure 6: Signal received under incandescent bulb.

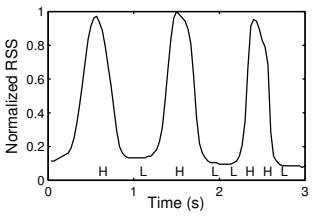

Figure 7: Signal received under variable speed.

willing to use this new type of channel would need more information to assess the feasibility of a potential application. For example, considering that the transmitters (lights in buildings, streets or roads) have a fixed output power and height, what symbol width should the designer use on objects to be able to decode information? And given this symbol width, what channel capacity can the designer expect? To provide some initial insights on these questions we gradually change the receiver's (and transmitter's) height from 20 cm to 55 cm. For each of these heights we test packets with different symbol widths, ranging from 1.5 cm to 7.5 cm. The packets are moved starting from a slow speed up to the maximum speed that allows the packets to be decodable. With this basic setup we identify two important trends:

Symbol width. Fig. 5(a) shows that there is a decodable region with a linear relationship between the maximum height of the transmitter/receiver and the symbol width. Assuming a constant power at the light source, there will be a point beyond which the receiver will not be able to decode information, no matter how long the symbol width is.

Throughput. For a given transmitter/receiver setup, the throughput is a function of the symbol width and the speed. Fixing one of these parameters determines the other. Using a constant speed of 8 cm/s, we identify the narrowest symbol width that makes the packet decodable. Fig. 5(b) shows that the channel's capacity decreases exponentially with the receiver's height.

Trends like the ones exposed above are important for the design of applications. Getting the receivers as close as possible to the moving objects would enable (i) smaller objects to be monitored, linear improvement in Fig. 5(a), and (ii) larger objects to provide exponentially more information, Fig. 5(b). But this evaluation is just a toy example. Central to our vision is the aim of formulating a solid theoretical framework to obtain initial parameters for a given lighting set up (road, street, building) without the need of performing prior in-situ evaluations. In the next section we describe an initial model that may enable us to achieve this.

Impact of other light sources. We also performed experiments using standard fluorescent lights and the sun. The decoding method still works in these settings but there are some important points to highlight. Fig. 6 presents the results using the fluorescent lights in our ceiling. The lights' height is 2.3 m and the receiver's is 0.2 m. Note that because we have an illuminated area, the noise floor is higher, which leads to a smaller difference between the `HIGH` and `LOW` symbols compared to our dark-room experiments. There is also a larger variance in the signal, 'thicker lines' than those in Fig. 4. This is due to the AC power supply [4].

The ceiling lights are significantly further away than the LED lamp used in our prior experiments, but due to their higher output power, we can still decode information. An extreme case highlighting the relationship between high output power and long distance coverage is the sun. The result is similar and omitted due to space limitation.

These experiments expose an important trade-off in our communication channel. In traditional communication systems, the transmitter and the sources creating interference are always independent, in our case they are the same. A light source with a high output power will increase the amount of light reflected towards the receiver (`HIGH` symbol) but it will also increase the noise floor. We require a theoretical framework to quantify precisely this trade-off in the Signal-to-Noise ratio (SNR) of our system.

3.2 Channel Distortion: Variable Speed

Thus far we have assumed an ideal scenario leading to a clean signal. In practice many events can distort the signal: rain, fog, damaged surfaces, dirt covering reflective materials, objects moving at variable speed, and so on. In these scenarios decoding the data may not be possible, but a plausible alternative is to transform the decoding problem into a classification problem. In scenarios where severe distortion is highly likely, we may not be able to decode bits after receiving the signal, but we could compare the distorted signal against a database of clean signals to see which one is the best match. Clearly, in this case we will not be able to use 2^N codes, with N being the number of bits. We will be constrained to use far less codes making sure that their inter Hamming distances are maximized (to have codes that are as different as possible from each other).

We now showcase a scenario where channel distortion is caused by objects moving at variable speeds. While many signal processing techniques could be used for classification problems, we use Dynamic Time Warping (DTW) to showcase our basic idea. DTW is a simple method used in many areas to measure the similarity of two signals. We use the two clean signals in Fig. 4 as the baselines for comparison. For the distorted signal we use the same packet as the one

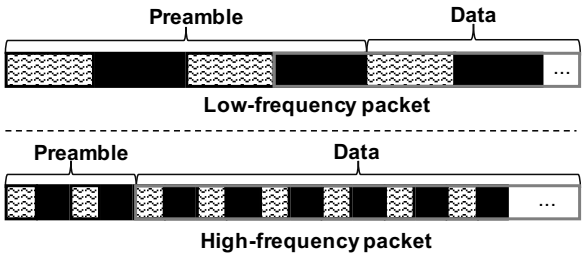

Figure 8: Illustration of the low-frequency and high-frequency packets.

in Fig. 4(b), but we change its speed. This packet moves at a certain speed when its first half (preamble) passes the receiver, and the speed is doubled when the second half (Data field) passes by. Figure 7 depicts the RSS of this distorted signal. The decoding method presented in the previous subsection leads to an erroneous symbol sequence when used on the distorted signal, "`HLHL.HL`", instead of the correct one "`HLHL.LHHL`". With DTW, the normalized distances between the signals in Fig. 7 and Fig. 4(a), and between Fig. 7 and Fig. 4(b) are 326 and 172, respectively (as a reference, the distance between the signal in Fig. 7 and itself is 131). Therefore, the distorted packet in Fig. 7 is classified as belonging to the same group as the packet in Fig. 4(b), which is right.

3.3 "Packet" Collisions: Frequency Domain

In the previous two subsections, we assume there is only one packet moving under the field of view of the receiver. In some scenarios this assumption will not hold. We now investigate the case where two packets move together and in parallel. We consider high- and low-frequency packets. A high-frequency packet is one with narrow symbol widths, so the received signal changes fast; and a low-frequency packet is one with wide symbol widths (slow-changing signal).

In our experiments both packets have the same length and their patterns are illustrated in Fig. 8. We carry out three different set ups: `Case1` – the field-of-view of the receiver covers more the low-frequency packet than the high frequency one (the low-frequency packet dominates the reflected light towards the receiver); `Case2` – the two packets exchange their positions (the high-frequency packet now becomes the dominator); `Case3` – the two packets share equally the receiver's filed of view (no dominant packet). The RSS captured at the receiver for these three cases are shown in Fig. 9(a), (c) and (e), respectively. For `Case1` and `Case2`, we were able to decode the bits using the decoding method presented in Sec. 3.1. For `Case3` however, we could not get accurate information from either method, decoding or DTW.

To obtain partial information for `Case3`, we use Fast Fourier Transforms (FFT) to analyze collisions in the frequency domain. The frequency spectrums are shown in Fig. 9(b), (d) and (f). In Fig. 9(b) and (d), we can observe a single dominant frequency, which explains why it was easy to decode information in the time domain. But the undecodable signal in Fig. 9(e) also benefits from the FFT, because we can detect the presence of two different types of object.

3.4 Noise Floor: LED as a Receiver

All the prior evaluations have not considered explicitly one of the most notorious problems with visible light systems: drastic changes in the noise floor. Normal changes in illumination conditions can lead to changes in noise floor that are

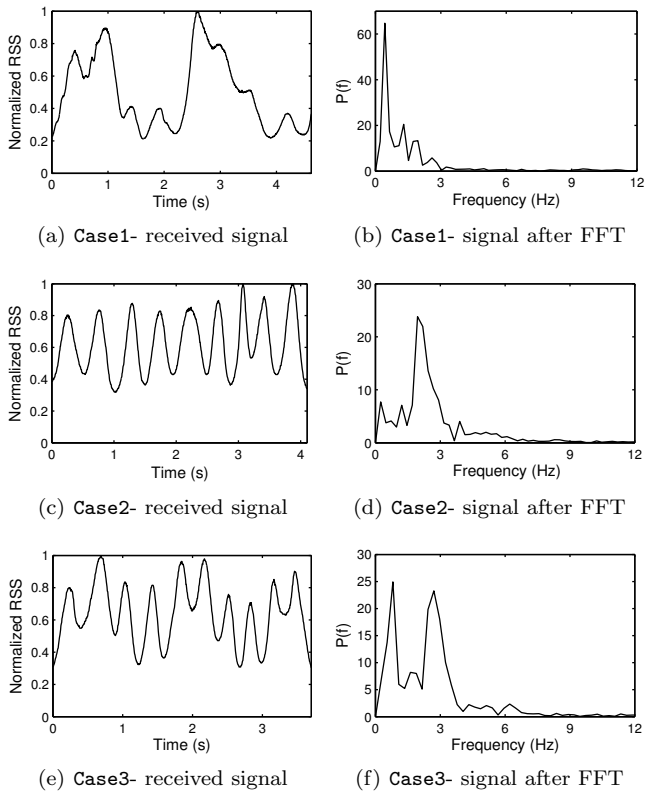

(a) `Case1`- received signal (b) `Case1`- signal after FFT

(c) `Case2`- received signal (d) `Case2`- signal after FFT

(e) `Case3`- received signal (f) `Case3`- signal after FFT

Figure 9: Captured signal and the transformation of these signals after FFT in a two-packet scenario.

Table 1: Supported noise floor (PD: photodiode).

Receiver	PD (`L1`)	PD (`L2`)	PD (`L3`)	LED
Saturation (lux)	960	1650	4500	>14300[1]

orders of magnitude higher than those experienced with radio. Photodiodes can be easily saturated under strong light conditions, especially outdoor with the sun. Recently, we have shown that for *active* visible light communications, i.e. when the light modulates the data, combining LEDs (acting as receivers) and photodiodes into a single sensor can overcome the problems related with the noise floor [16]. We will investigate this same idea for the *passive* case. To make our new communication system work in a stable manner under various light conditions, we will design a receiver that can switch dynamically - even within the same symbol period - to the best suited sensor, photodiode or LED.

To highlight the trade-off posed by photodiodes and LEDs acting as receivers, we perform some experiments to quantify their sensitivity. The sensitivity of photodiodes can be adjusted from a high sensitivity (long range but easily saturated) to a low sensitivity (short range but more resilient to saturation). The experimental results are shown in Table 1. We observe that when the photodiode works at sensitivity level `L1` (corresponding to long reception range), it saturates at 960 lux, which maps roughly to a well illuminated room. At `L3` (corresponding to short reception range), the photodiode works for noise floor values up to 4500 lux. The LED,

[1]We use an android phone to measure the light intensity and the maximal light intensity it supports is 14300 lux.

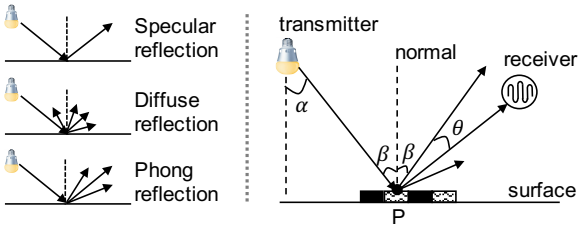

Figure 10: Light reflections: (left) illustration of different reflections; (right) detailed Phong reflection.

however, can work when the noise floor is higher than 14,300 lux. In outdoor scenarios with daylight, the intensity can easily be higher than 10,000 lux. In indoor scenarios, the light intensity is normally around several hundreds lux with artificial lighting and around several thousands lux near windows. Thus, to have an "all-terrain" system, it will be necessary to have a multi-purpose LED-photodiode receiver.

4. PRELIMINARY ANALYTICAL MODEL

In this section we describe the initial steps we are taking to derive a theoretical framework for our new channel. The explanation of our model is divided into three components: light attenuation, light reflection and light reception.

Light attenuation. The light emitted by LEDs decays in intensity based on two main factors: distance traveled and irradiation angle. The light received by a photosensor is inversely proportional to the power of the distance traveled by the light beam. This attenuation follows the basic laws of physics. But LED light is further attenuated by the irradiation angle (α in Fig. 10). The light intensity emitted by the LED bulb is proportional to the cosine of the irradiation angle. This radial attenuation is captured by the well-known Lambertian emission law [2]. In our model we include these two effects (distance and angle) to estimate the amount of light reaching a particular point.

Light reflection. Once a light beam is emitted by an LED, it will be absorbed and reflected by surrounding objects. Upon impinging an object, only a fraction of the light will be reflected, the rest is absorbed. The amount of reflected light is dictated by the reflection coefficient ρ of the material, which takes values in the range $[0, 1]$. Also, depending on how smooth the material's surface is, we will observe two types of reflections: specular and diffused. Specular reflection occurs on smooth mirror-like surfaces, while reflections on rough surfaces are normally diffused. Illustrations of these reflections are presented in Fig. 10(left). The ruggedness of a material is captured by the shininess parameter n, which can take values between 1 and ∞, the higher the value the smoother the surface.

Light reception. Based on the attenuation and reflection properties of light presented above, our analytical model is built upon the empirically based Phong reflection model [11]. This model describes how a surface reflects lights as a combination of diffuse and specular reflections. We first present the basic Phong model and then describe our extensions.

Basic Phong model. Consider a single light ray impinging on the surface of a material whose reflection and shininess coefficients are denoted by ρ and n. As shown in Fig. 10(right), let α and β be the irradiation and incidence angles, and θ be the angle between the reflected light and the direction pointing from the reflecting point P to the receiver. We want to identify the amount of light irradiating from the impinging

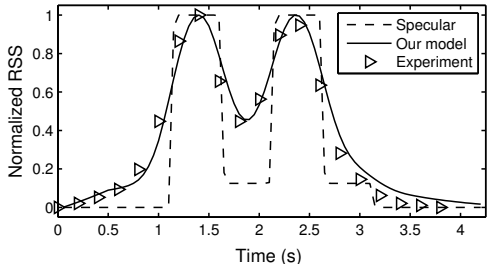

Figure 11: Preliminary model validation: analytical results vs. experimental result.

point P and going towards the direction of the receiver. Denoting k_a as the ambient light component at P, and k_s and k_d as the fractions of the impinging light transformed into specular and diffused reflections, respectively. Then, the reflected light towards the receiver h_r under the basic Phong model is given by [11]:

$$h_r = k_a + \rho \cdot (k_d \cdot \cos\beta + k_s \cdot \cos^n \theta) \quad (1)$$

Our system's model. In our communication system, we consider three materials: the ground (`G`), a high reflective material (`H`) and a low reflective material (`L`). The high and low reflective materials are used to build the barcodes. Each material j has a tuple $< \rho_j, n_j, k_{d,j}, k_{s,j} >$ quantifying its reflective properties. To obtain the RSS at a receiver, we focus on the area covered by the field-of-view of the photosensor at a given point in time. We divide this area in tiny cells of size 2.3-by-2.3 mm (this size is used to match the sensing area of our photodiode). The light emitted by the LED, and impinging on the field-of-view area, is transformed into a set of rays $\mathcal{I}$. According to the basic Phong model (1), for each light ray $i \in \mathcal{I}$, its corresponding reflection towards the receiver $h_{r,i}$ is given by:

$$h_{r,i} = k_a + \rho_i \cdot (k_{d,i} \cdot \cos\beta_i + k_{s,i} \cdot \cos^{n_i} \theta_i),\ i \in \mathcal{I} \quad (2)$$

where $\rho_i \in \{\rho_H, \rho_L, \rho_G\}$ and its value is chosen based on the material where the ray i is impinging on. Similar rules apply to n_i, $k_{d,i}$ and $k_{s,i}$. The angles β_i and θ_i are calculated based on the positions of the transmitter and receiver. Given the contributions of each light ray i in (2), and the well-known methods used to account for signal attenuation (described at the beginning of this section), the RSS at the receiver is calculated by summing up the contributions of each ray $i \in \mathcal{I}$. A preliminary validation of our model is given in Fig. 11, where we compare the results of one of our measurements with the model and observe a close fit. For the sake of comparison, we also use the model to estimate what would the outcome be if all reflection would be specular, which is what commercial barcode readers (based on laser) observe at short distances. The results show a perfect square wave, which is not only a much easier signal to decode but one that will not be exposed to distortions, multi-barcode collisions or affected by sunlight.

5. RELATED WORK

Backscatter communication. An important aspect of our system is that light sources are modulated by reflective surfaces. This concept is inspired by backscatter communication, where passive tags modulate the electromagnetic waves produced by external sources. This technique has been traditionally used by RFID tags [18], and recently

applied to other radio technologies, such as Wi-Fi [3] and TV signals [9], as well as visible light technology [6] (where semi-passive tags are powered by solar cells). In the same way radio-backscatter exploits the surrounding radio waves in our environments to provide 'out of thin air' communication, we want to exploit visible light waves. Where possible we will build on top of advances of radio-backscatter but it is important to highlight that (i) visible light waves have completely different properties than radio waves, and (ii) our tags (packets) are not electronic devices and use no power at all (which is different from [6]).

Barcodes. Grocery stores, production inventory and tracking use barcodes as identification system. In spirit this system is similar to ours, but it is not exposed to the same challenges. Systems using lasers or LEDs as scanners and photosensors or charge couple devices (CCD) as detectors have been developed to decode barcodess [13, 10]. These systems are designed to operate with the transmitter and receiver at the same position, using very coherent light sources (like laser), and without considering distortions. These operational requirements are stringent and differ from the more generic scenario investigated in our system: (i) independent components (transmitter, receiver, packet) having no control over each other, and relying on the objects' mobility to operate, (ii) generic non-coherent light sources at long distances, which increase the amount of diffused light (noise), and (iii) various distortion effects like variable speeds, dirt or fog.

VLC and sensing. By modulating the light intensity emitted by LEDs, visible light has been exploited for communication and has attracted large attention for next-generation wireless networks [14, 19]. More recently, interest has spawn for visible light sensing in human motions [8], mobile interaction [20], localization [7], among other topics. These works fall in the category of low-end VLC implementations. Our work differs from these sensing systems on the basic fact that we do not use modulated light sources. Instead, we embed data into reflecting objects. Our proposed system has the potential to build a different (parallel) passive VLC system. Other VLC studies use cameras as receivers for human-computer interaction [15], visual MIMO [1] and localization [5]. Cameras are power hungry, more complex and pose threats to user's privacy. For these reasons, we use simple photodetectors as receivers in our system. *There is one area however where we expect to benefit greatly from VLC: next-generation visible light receivers.* VLC is improving the sensitivity and operational range of photodiodes to increase the capacity, coverage and robustness of active links. These same characteristics (sensitivity and operational range) will also improve the performance of our passive system.

6. DISCUSSION AND CONCLUSION

Considering all the light sources in our surroundings, we envision a future with *distributed and large-scale barcode systems for our cities and buildings*, where we could monitor coarse-grained events (i) by deploying a large number of small boxes (smart photosensors), and (ii) by 'dressing' objects of interest with different reflective surfaces. To achieve this vision, we proposed a passive communication system for visible light signals. We identified several challenges and evaluated them preliminary through experiments and analysis, but there is much more to do. We are currently working on extending this work on three main fronts:

Deeper analysis. Based on the Phong reflection model, we are deriving a framework to estimate the channel capacity theoretically and to provide an analytical tool to assess the feasibility of our ideas in real scenarios.

More robust methods. As an initial step, we used basic methods to encode and to obtain information (Manchester encoding, DTW, FFT). We are evaluating other methods from communication theory and signal processing, to identify the mechanisms that are best suited for our new channel.

Coexistence with active VLC. In the future many LEDs will emit modulated light, which could enable applications such as passive and accurate localization with visible light. Achieving this goal requires designing a receiver that can jointly process active and passive information.

7. REFERENCES

[1] Ashok, A., Gruteser, M., Mandayam, N., Silva, J., Varga, M., and Dana, K. Challenge: Mobile optical networks through visual mimo. In *MobiCom* (2010).

[2] Kahn, J., and Barry, J. Wireless infrared communications. *Proceedings of the IEEE* (1997).

[3] Kellogg, B., Parks, A., Gollakota, S., Smith, J. R., and Wetherall, D. Wi-fi backscatter: Internet connectivity for rf-powered devices. In *SIGCOMM* (2014).

[4] Kuo, Y.-S., Pannuto, P., and Dutta, P. System architecture directions for a software-defined lighting infrastructure. In *VLCS* (2014).

[5] Kuo, Y.-S., Pannuto, P., Hsiao, K.-J., and Dutta, P. Luxapose: Indoor positioning with mobile phones and visible light. In *MobiCom* (2014).

[6] Li, J., Liu, A., Shen, G., Li, L., Sun, C., and Zhao, F. Retro-VLC: Enabling Battery-free Duplex Visible Light Communication for Mobile and IoT Applications. In *HotMobile* (2015).

[7] Li, L., Hu, P., Peng, C., Shen, G., and Zhao, F. Epsilon: A visible light based positioning system. In *NSDI* (2014).

[8] Li, T., An, C., Tian, Z., Campbell, A. T., and Zhou, X. Human sensing using visible light communication. In *MobiCom* (2015).

[9] Liu, V., Parks, A., Talla, V., Gollakota, S., Wetherall, D., and Smith, J. R. Ambient backscatter: Wireless communication out of thin air. *SIGCOMM CCR* (2013).

[10] Massieu, J.-L., and Puech, J.-M. Optoelectronic device for acquisition of images, in particular of bar codes, Aug. 20 2002. US Patent 6,435,411.

[11] Phong, B. T. Illumination for computer generated pictures. *Communications of the ACM* (1975).

[12] Proakis, J., and Salehi, M. *Fundamentals of Communication Systems*. Pearson Education, 2007.

[13] Roustaei, A. Optical scanning head, Oct. 11 1994. US Patent 5,354,977.

[14] Tsonev, D., Videv, S., and Haas, H. Light fidelity (Li-Fi): towards all-optical networking. In *SPIE* (2013).

[15] Wachs, J. P., Kölsch, M., Stern, H., and Edan, Y. Vision-based hand-gesture applications. *Communications of the ACM* (2011).

[16] Wang, Q., Giustiniano, D., and Gnawali, O. Low-cost, flexible and open platform for visible light

communication networks. In *HotWireless* (2015).

[17] Wang, Q., Giustiniano, D., and Puccinelli, D. An open-source research platform for embedded visible light networking. *IEEE Wireless Communication* (2015).

[18] Want, R. Enabling ubiquitous sensing with rfid. *IEEE Computer* (2004).

[19] Wu, S., Wang, H., and Youn, C.-H. Visible light communications for 5G wireless networking systems: from fixed to mobile communications. *IEEE Network* (2014).

[20] Zhang, C., Tabor, J., Zhang, J., and Zhang, X. Extending mobile interaction through near-field visible light sensing. In *MobiCom* (2015).